

Heat Transfer Enhancement in 2D Magnetohydrodynamic Channel Flow by Boundary Feedback Control

Lixiang Luo and Eugenio Schuster

Abstract—The interaction between an electrically-conducting fluid in a channel flow and an imposed transverse magnetic field generates significant magnetohydrodynamics (MHD) effects, which often result in higher pressure gradients and lower heat transfer rates. The later effect is particularly undesirable in cooling-system applications. A nonlinear Lyapunov-based boundary control law is proposed for mixing and heat transfer enhancement in a magnetohydrodynamic (MHD) channel flow, also known as Hartmann flow. A direct numerical simulation (DNS) code has been developed to simulate the full MHD equations and the heat transfer equation. A numerical study shows the effectiveness of the proposed controller.

I. INTRODUCTION

While control of flows has been an active area for several decades now, up until now active feedback flow control developments have had little impact on electrically conducting fluids moving in electromagnetic fields. Active feedback control in electrically conducting flows, implemented through micro-electro-mechanical or micro-electro-magnetic actuators and sensors, can be used to achieve optimally the desired level of stability (when suppression of turbulence is desired) or instability (when enhancement of mixing is desired). As a result, a small amount of active control applied to magnetohydrodynamic (MHD) flows, magnetogasdynamic (MGD) flows, and plasma flows can dramatically change their equilibrium profiles and stability (turbulence fluctuations) properties. These changes influence heat transfer, hydrodynamic drag, pressure drop, and the required pumping power for driving the fluid.

Prior work in this area focuses mainly on electro-magneto-hydro-dynamic (EMHD) flow control for hydrodynamic drag reduction, through turbulence control, in weak electrically conducting fluids such as saltwater. Traditionally two types of actuator designs have been used: one type generates a Lorentz field parallel to the wall in the streamwise direction, while the other type generates a Lorentz field normal to the wall in the spanwise direction. EMHD flow control has been dominated by strategies that either permanently activate the actuators or pulse them at arbitrary frequencies. However, it has been shown that feedback control schemes, making use of “ideal” sensors, can improve the efficiency, by reducing control power, for both streamwise [1] and spanwise [2], [3] approaches. From a model-based-control

point of view, feedback controllers for drag reduction are designed in [4], [5] using distributed control techniques based on linearization and model reduction.

In this work we focus our attention on MHD flows, where the fluid is incompressible and Newtonian (constant viscosity). We are interested in one of the main applications of MHD flows: liquid-metal cooling systems. Due to their excellent thermal and physical properties (high boiling point and thermal conductivity), liquid metals are ideal for high heat flux dissipation. Liquid metals have been considered as coolants for more than five decades, particularly in the nuclear fission reactor industry. The possible usage of liquid metals as self-cooled blankets in magnetic confinement nuclear fusion reactors has been in consideration for the past 30 years. Liquid-metal cooling systems have also recently attracted an increased interest in the fast growing computer industry.

In a fusion reactor, the main function of the coolant is the absorption of energy from the neutron flux and the transfer of heat to an external energy conversion system. In addition, if a breeder liquid metal such as liquid-lithium is considered, the blanket can also carry out the breeding of tritium, which is part of the fuel used by the reactor. Unfortunately, the flow is affected by the strong magnetic field used to confine the plasma inside the reactor. When an electrically conducting fluid moves in the presence of a transverse magnetic field, it produces an electrical current due to charge separation. The interaction between this induced electric current and the imposed magnetic field originates a body force, called the Lorentz force, which acts on the fluid itself in the opposite direction of the fluid motion. As a consequence, pressure drop has to be increased to maintain the mean velocity of the flow, which requires more power to pump the liquid through the cooling-system ducts. In addition, this force tends to confine vorticity and stabilize the flow, reducing the heat transfer rate significantly. These MHD effects prevent liquid-metal cooling systems from producing the heat transfer improvements which might be expected based on the much higher thermal conductivity of the coolant. Research programs worldwide have been traditionally engaged in the study of the effects of the magnetic field on heat transfer and hydrodynamic drag through modeling and experimentation. However, in general only passive turbulence and heat-transfer promoters were considered.

In this work we consider a Hartmann flow, an electrically conducting incompressible fluid moving between parallel plates through an imposed transverse magnetic field. Active feedback boundary control is used to improve mixing and

This work was financed (in part) by a grant from the Commonwealth of Pennsylvania, Department of Community and Economic Development, through the Pennsylvania Infrastructure Technology Alliance (PITA). L. Luo and E. Schuster are with the Department of Mechanical Engineering and Mechanics, Lehigh University, 19 Memorial Drive West, Bethlehem, PA 18015-1835, USA (lil19@lehigh.edu, schuster@lehigh.edu).

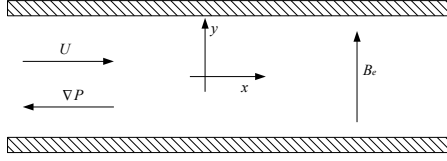


Fig. 1. 2D MHD flow between plates

heat transfer by enhancing the instability of the Hartmann flow profile. From the point of view of controls, we follow the ideas introduced in a previous work by one of the authors [6]. Pressure sensors, magnetic field sensors, and micro-jets embedded into the walls of the flow domain are used to implement the feedback control law. A numerical study of the effectiveness of the proposed controller, which was still pending, is presented in this paper. The considered system and control design require a numerical method handling the coupled MHD equations, without neglecting any component of the magnetic field. In addition, the heat transfer equation is incorporated into the MHD model with the ultimate goal of assessing the impact of the proposed feedback controller on the heat transfer properties of the channel.

The paper is organized as follow. Section II introduces the governing equations of our system. The equilibrium solution is presented in Section III. The magnetohydrodynamic effects are discussed in Section IV. The controller is introduced in Section V, where the Lyapunov analysis for the designed boundary control law is presented. The numerical method used to simulate the system is discussed in Section VI. An in-depth analysis of simulation results is carried out in Section VII. Section VIII closes the paper stating the conclusion and the identified future work.

II. GOVERNING EQUATIONS

We consider a 2D, incompressible, electrically conducting fluid flowing between two parallel plates ($0 \leq x \leq d = 4\pi$, and $-1 \leq y \leq 1$) along the x -direction, as illustrated in Fig. 1, where an external magnetic field B_e is imposed perpendicularly to the plates, i.e., in the y -direction. This flow was first investigated experimentally and theoretically by Hartmann [7]. The mass flux Q is fixed. A uniform pressure gradient P_x in the x -direction is required to balance the boundary drag force and the body force due to the MHD effects. In addition, the bottom and top plates have different fixed temperatures T_b and T_p respectively. Space variables x and y , time t , velocity \mathbf{v} , magnetic induction \mathbf{B} and temperature T are converted to their dimensionless form: $x = x^*/L$, $y = y^*/L$, $t = t^*U_0/L$, $\mathbf{B} = \mathbf{B}^*/B_0$, $\mathbf{v} = \mathbf{v}^*/U_0$, $T = T^*/T_0$, where L , U_0 , B_0 and T_0 are dimensional reference length, velocity, magnetic field and temperature. Variables denoted by the star notation are dimensional quantities. The vector variables are defined as

$$\mathbf{v}(x, y, t) = U(x, y, t)\hat{x} + V(x, y, t)\hat{y} \quad (1)$$

$$\mathbf{B}(x, y, t) = B^u(x, y, t)\hat{x} + B^v(x, y, t)\hat{y} \quad (2)$$

where \hat{x} and \hat{y} are unit vectors on x and y directions. The dimensionless governing equations for the MHD channel

flow are given by

$$\frac{\partial \mathbf{v}}{\partial t} = \frac{1}{\text{Re}} \nabla^2 \mathbf{v} - \nabla P - (\mathbf{v} \cdot \nabla) \mathbf{v} - \text{Al} [(\nabla \times \mathbf{B}) \times \mathbf{B}] \quad (3)$$

$$\frac{\partial \mathbf{B}}{\partial t} = \frac{1}{\text{Re}_m} \nabla^2 \mathbf{B} + (\mathbf{B} \cdot \nabla) \mathbf{v} - (\mathbf{v} \cdot \nabla) \mathbf{B} \quad (4)$$

$$\nabla \cdot \mathbf{v} = 0 \quad (5)$$

$$\nabla \cdot \mathbf{B} = 0 \quad (6)$$

$$\frac{\partial T}{\partial t} = \frac{1}{\text{Pe}} \nabla^2 T + (\mathbf{v} \cdot \nabla) T \quad (7)$$

The characteristic numbers, including Reynolds number, Magnetic Reynolds number, Alfvén number and Péclet number are defined as: $\text{Re} = U_0 L / \nu$, $\text{Re}_m = \mu \sigma U_0 L$, $\text{Al} = B_0^2 / (\mu \rho U_0^2)$, $\text{Pe} = \rho c_p U_0 L / \lambda$. The physical properties of the fluid, including the mass density ρ , the dynamic viscosity ν , the electrical conductivity σ , the magnetic permeability μ , the specific heat c_p , and the thermal conductivity λ , are all assumed constant.

The boundary conditions for this uncontrolled MHD system are

$$\begin{aligned} U(x, \pm 1, t) &= 0, & V(x, \pm 1, t) &= 0, \\ B^u(x, \pm 1, t) &= 0, & \left. \frac{\partial B^v}{\partial y} \right|_{y=\pm 1} &= 0, \\ T(x, -1, t) &= T_b, & T(x, 1, t) &= T_p. \end{aligned}$$

Periodic boundary conditions are used for the streamwise direction, which is automatically fulfilled by the pseudo-spectrum method (see Section VI).

III. EQUILIBRIUM SOLUTIONS

For a 2D channel with constant height, as the one depicted in Fig. 1, a fully developed equilibrium flow is established. In this case, the flow velocity has only one component, which depends on the coordinate y , i.e., $\mathbf{v} = \bar{U}(y)\hat{x}$. The magnetic field is decomposed into two contributions, one due to the external imposed magnetic field and the other caused by the magnetic field induced by the flow $\mathbf{B} = \mathbf{B}_e + \bar{\mathbf{B}}_i = B_e \hat{y} + \bar{\mathbf{B}}_i$. Substituting this expression for the magnetic field \mathbf{B} into equation (4) shows that the only component of the induced magnetic field is $\bar{\mathbf{B}}_i = \bar{B}^u(y)\hat{x}$. The system equations reduce to

$$\frac{1}{\text{Re}_m} \frac{\partial^2 \bar{B}^u}{\partial y^2} + B_e \frac{\partial \bar{U}}{\partial y} = 0 \quad (8)$$

$$\frac{1}{\text{Re}} \frac{\partial^2 \bar{U}}{\partial y^2} + \text{Al} B_e \frac{\partial \bar{B}^u}{\partial y} = P_x, \quad (9)$$

with boundary conditions

$$\bar{U} = 0, \quad \bar{B}^u = 0 \quad \text{at} \quad y = \pm 1. \quad (10)$$

Since the mass flux is assumed to be constant, it is more convenient to write the solution in terms of the mass flux Q . From the integral relation

$$\int_{-1}^1 \bar{U}(y) dy = Q, \quad (11)$$

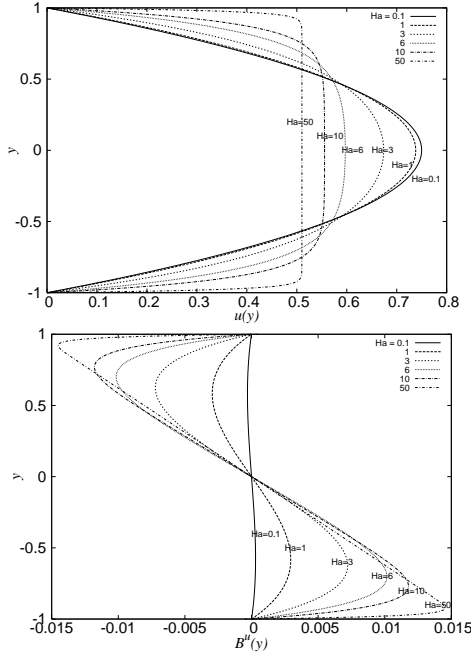


Fig. 2. Velocity (top) and induced magnetic field (bottom) profiles for perfectly insulating walls ($Re = 10000$, $Al = 0.01$, $Re_m = 0.1$, $Q = 1$.)

it is possible to obtain the pressure gradient P_x , given by

$$P_x = \frac{B_e}{\frac{2}{\tanh(Ha)} - \frac{2}{Ha}} \sqrt{\frac{Al Re_m}{Re}} Q. \quad (12)$$

Hence, the equilibrium solution can be written as

$$\bar{U}(y) = \frac{Q}{2 - \frac{2}{Ha} \tanh(Ha)} \left[1 - \frac{\cosh(Ha y)}{\cosh(Ha)} \right] \quad (13)$$

$$\bar{B}^u(y) = \sqrt{\frac{Re_m}{Al Re}} \frac{Q}{\frac{2}{\tanh(Ha)} - \frac{2}{Ha}} \left[\frac{\sinh(Ha y)}{\sinh(Ha)} - y \right], \quad (14)$$

where $Ha = B_e \sqrt{Al Re Re_m}$ is called the Hartmann number. Fig. 2 shows the velocity and the induced magnetic field equilibrium profiles for different Hartmann numbers.

At the equilibrium, the temperature distribution is linear, regardless of the velocity profile. For the boundary conditions used in simulations ($T_b = 1$, $T_p = 0.6$), the solution is

$$T = -0.2y + 0.8 \quad (15)$$

Since the vertical component of velocity at the boundaries is zero, the heat flux is determined by the conduction term, which is simply proportional to the temperature gradient at the boundary. In this linear case, the temperature gradient is 0.2.

IV. MAGNETOHYDRODYNAMIC EFFECTS

When $B_o = 0$ ($Al = 0$), the momentum equation (3) reduces to the well-known Navier-Stokes equation. The two-dimensional channel flow, also known as the Poiseuille flow, is frequently cited as a paradigm for transition to turbulence, and has drawn extensive attention through the history of fluid dynamics. This is a classical flow control problem that has been studied in [8] and the references therein assuming the

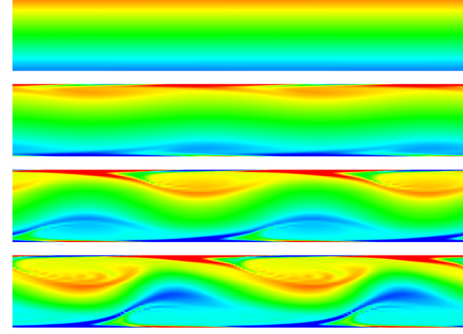


Fig. 3. Vorticity maps for ($Re = 7500$, $t = 0, 1262, 1682, 4485$)

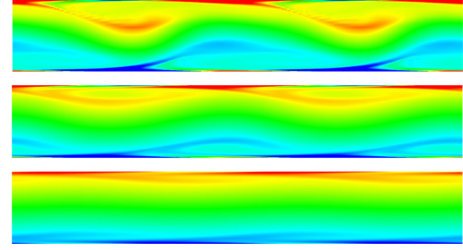


Fig. 4. Vorticity maps after the magnetic field being imposed ($Re = 7500$, $Be = 0.3$, $t = 140, 285, 374$)

availability of an array of pressure sensors on the walls and an array of MEMS micro-jet actuators (also distributed along the walls) capable of blowing/suction in the wall-normal direction. Incompressible conventional flows in 2D channels can be stable for low Reynolds numbers, as infinitesimal perturbations in the flow field are damped out. The flows turn linearly unstable for high Reynolds numbers $Re > 5772$ [9]. Such flows usually reach statistically steady states, which we call fully established flows. Simulation results are presented in Fig. 3 to show how a channel flow ($Re = 7500$) develops to a fully established flow. The initial velocity profile is the parabolic equilibrium solution of the Navier-Stokes equation, which is linearly unstable for this Reynolds number. Fig. 3 shows how the vorticity map evolves in time until reaching a fully established flow when the initial equilibrium velocity profile is infinitesimally perturbed at $t = 0$. When $B_o \neq 0$, vorticity maps, obtained through direct numerical simulation studies, show in Fig. 4 the stabilizing effect of the imposed transverse magnetic field on the 2D Hartmann flow. The simulation is started at $t = 0$ with the fully established flow achieved in Fig. 3.

V. BOUNDARY CONTROL OF MIXING

We choose the energy function

$$E(\mathbf{v}, \mathbf{B}) = \int_{-1}^1 \int_0^d k_1 (u^2 + v^2) + k_2 (b^{u^2} + b^{v^2}) dx dy, \quad (16)$$

where k_1 and k_2 are constant weights, and u , v , b^u , and b^v are the deviation variables defined as

$$\begin{aligned} u &= U - \bar{U}, & v &= V - \bar{V} = V \\ b^u &= B^u - \bar{B}^u, & b^v &= B^v - \bar{B}^v = B^v - B_e, \\ p &= P - \bar{P}. \end{aligned}$$

We apply control in the wall normal direction

$$u(x, -1, t) = u(x, 1, t) = 0 \quad (17)$$

$$v(x, -1, t) = v(x, 1, t) = v_{wall}(x, t), \quad (18)$$

and measure the wall normal component of the induced magnetic field

$$b^u(x, -1, t) = b^u(x, 1, t) = 0 \quad (19)$$

$$b^v(x, -1, t) = b_{bot-wall}^v(x, t), \quad b^v(x, 1, t) = b_{top-wall}^v(x, t). \quad (20)$$

Taking into account our boundary conditions, the time derivative of $E(\mathbf{v}, \mathbf{B})$ along the trajectories can be written as

$$\begin{aligned} \dot{E}(\mathbf{v}, \mathbf{B}) = & -\frac{1}{\text{Re}} m(\mathbf{v}, \mathbf{B}) \\ & - \int_0^d v_{wall} \left[k_1 \Delta p + k_2 \frac{\Delta[(b^v)^2]}{2} \right] dx + g(\mathbf{v}, \mathbf{B}), \end{aligned} \quad (21)$$

where

$$\begin{aligned} m(\mathbf{v}, \mathbf{B}) = & k_1 \int_{-1}^1 \int_0^d (u_x^2 + u_y^2 + v_x^2 + v_y^2) dx dy \\ & + k_2 \frac{\text{Re}}{\text{Re}_m} \int_{-1}^1 \int_0^d ((b_x^u)^2 + (b_y^u)^2 + (b_x^v)^2 + (b_y^v)^2) dx dy, \end{aligned} \quad (22)$$

$$\Delta p = p(x, 1, t) - p(x, -1, t) \quad (23)$$

$$\Delta[(b^v)^2] = (b^v(x, 1, t))^2 - (b^v(x, -1, t))^2 \quad (24)$$

and the function $g(\mathbf{v}, \mathbf{B})$ satisfies

$$\begin{aligned} |g(\mathbf{v}, \mathbf{B})| \leq & g_1 m(\mathbf{v}, \mathbf{B}) + g_2 m^2(\mathbf{v}, \mathbf{B}) + g_3 \int_0^d v_{wall}^2 dx \\ & + g_4 \int_0^d (b_{top-wall}^v)^2 dx + g_5 \left(\int_0^d (b_{top-wall}^v)^2 dx \right)^2 \end{aligned} \quad (25)$$

where g_1, g_2, g_3, g_4 and g_5 are constants conveniently defined.

The stretching of material elements accompanied by folding are keys to effective mixing. The measure (22) seems to be strongly connected to mixing since there is a direct relation between stretching of material elements and the spatial gradients of the flow field. Folding is present implicitly in (22) due to the boundedness of the flow domain and the fact that \mathbf{v} satisfies the Navier-Stokes equation. The design goal is a feedback control law, in terms of suction and blowing of fluid normally to the channel wall, that is optimal with respect to some meaningful cost functional related to $m(\mathbf{v}, \mathbf{B})$.

Theorem 1: The cost functional

$$J(v_{wall}) = \lim_{t \rightarrow \infty} \left[2\beta E(\mathbf{v}(t), \mathbf{B}(t)) + \int_0^t h(\mathbf{v}(\tau), \mathbf{B}(\tau)) d\tau \right]$$

where

$$\begin{aligned} h(\mathbf{v}, \mathbf{B}) = & \frac{2\beta}{\text{Re}} m(\mathbf{v}, \mathbf{B}) - 2\beta [g(\mathbf{v}, \mathbf{B}) \\ & + g_4 \int_0^d (b_{top-wall}^v)^2 dx + g_5 \left(\int_0^d (b_{top-wall}^v)^2 dx \right)^2] \\ & - \beta \int_0^d v_{wall}^2 dx - \beta \int_0^d \left[k_1 \Delta p + k_2 \frac{\Delta[(b^v)^2]}{2} \right]^2 dx \end{aligned} \quad (26)$$

is maximized by the control

$$v_{wall} = - \left[k_1 \Delta p + k_2 \frac{\Delta[(b^v)^2]}{2} \right]. \quad (27)$$

Moreover, solutions of the system described by the dimensionless perturbation equations satisfy

$$\begin{aligned} h(\mathbf{v}, \mathbf{B}) \leq & l_1 m(\mathbf{v}, \mathbf{B}) + l_2 m^2(\mathbf{v}, \mathbf{B}) - l_3 \int_0^d v_{wall}^2 dx \\ & - \beta \int_0^d \left[k_1 \Delta p + k_2 \frac{\Delta[(b^v)^2]}{2} \right]^2 dx \end{aligned} \quad (28)$$

for arbitrary values of control v_{wall} and with

$$l_1 = 2\beta \left(\frac{1}{\text{Re}} + g_1 \right), \quad l_2 = 2\beta g_2, \quad l_3 = \beta - g_3. \quad (29)$$

Proof. Using (21), we can write equation (26) as

$$\begin{aligned} h(\mathbf{v}, \mathbf{B}) = & -2\beta \dot{E}(\mathbf{v}, \mathbf{B}) - 2\beta g_4 \int_0^d (b_{top-wall}^v)^2 dx \\ & - 2\beta g_5 \left(\int_0^d (b_{top-wall}^v)^2 dx \right)^2 \\ & - \beta \int_0^d \left(v_{wall} + \left[k_1 \Delta p + k_2 \frac{\Delta[(b^v)^2]}{2} \right] \right)^2 dx. \end{aligned} \quad (30)$$

In addition, the cost functional can be written as

$$\begin{aligned} J(v_{wall}) = & 2\beta E(\mathbf{v}(0), \mathbf{B}(0)) \\ & - 2\beta \lim_{t \rightarrow \infty} \left[g_4 \int_0^t \int_0^d (b_{top-wall}^v)^2 dx d\tau \right. \\ & \left. - g_5 \int_0^t \left(\int_0^d (b_{top-wall}^v)^2 dx \right)^2 d\tau \right] \\ & - \beta \lim_{t \rightarrow \infty} \int_0^t \int_0^d \left(v_{wall} + \left[k_1 \Delta p + k_2 \frac{\Delta[(b^v)^2]}{2} \right] \right)^2 dx d\tau. \end{aligned}$$

The cost functional is maximized when the last integral is zero. Therefore the control (27) is optimal. In addition, replacing the expression (21) for $\dot{E}(\mathbf{v}, \mathbf{B})$ in equation (30) and using (25) we can obtain (28) [6]. \square

Inequality (28) implies that $h(\mathbf{v}, \mathbf{B})$ cannot be made large without making $m(\mathbf{v}, \mathbf{B})$ large as long as the constant β is chosen to make $k_3 > 0$. Thus, the control law (27) maximizes mixing, with minimal control (v_{wall}) and sensing $(\Delta p, \Delta[(b^v)^2])$ effort.

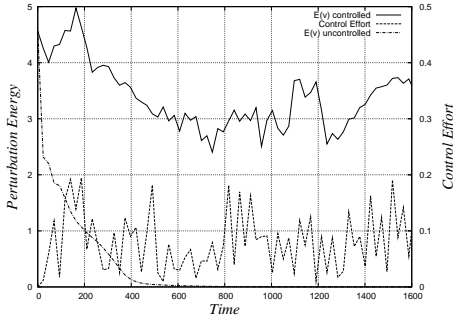


Fig. 5. Perturbation energy and control effort ($Re=7500, B_e=0.3$)

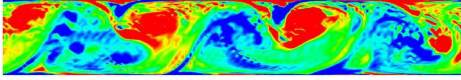


Fig. 6. Vorticity maps ($Re=7500, B_e=0.3, t=140$)

VI. NUMERICAL METHOD

A direct numerical simulation (DNS) code based on the full MHD equations is necessary in this case to allow the measurement of the induced magnetic field at the boundary, as is required by the proposed control law (27). Exploiting the similar structures of the Navier-Stokes and magnetic induction equations, our approach to the problem was to integrate the equations on a staggered grid within a periodic channel flow geometry using a hybrid Fourier pseudospectral–finite difference discretization and the fractional step technique. This technique had been already proved appropriate for time-accurate simulation of both laminar and turbulent flows at low Reynolds number in conventional incompressible channel flows. In this work we extended this technique by incorporating the magnetic induction equation and the divergence-free condition for the magnetic field. Taking advantage of the periodic boundary conditions in the streamwise (x) direction, this direction is discretized using Fourier pseudospectral methods [10]. The variables of the system are discretized in the x -direction using the Fourier transform, and the periodic boundary conditions in the streamwise direction are automatically fulfilled. The wall-normal (y) direction is discretized using central finite difference on a non-uniform staggered grid [11]. Experience has shown that numerical oscillations occur in incompressible flow simulations when streamwise and spanwise components of the velocity are defined on the same grid points.

The equations are integrated in time using a fractional step method [12], designed to ensure the fulfillment of the divergence-free conditions, based on a hybrid explicit-implicit time discretization [13]. The nonlinear terms are integrated explicitly using a fourth-order, low-storage Runge-Kutta method, while the viscous terms are treated implicitly using the Crank-Nicolson method.

VII. SIMULATION RESULTS

In this section, we study the effectiveness of the proposed control law (27) for mixing and heat transfer enhancement. All the simulations are carried out for the same flow domain ($0 \leq x \leq d = 4\pi, -1 \leq y \leq 1$). The same mesh is used in

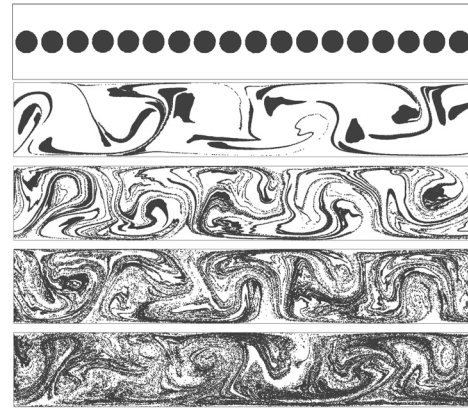


Fig. 7. Particle distribution for controlled flow ($Re = 7500, B_e = 0.3, t = 0, 10, 34, 58, 115$)

all the simulations presented in this section (grid points in the x direction: $NX = 150$, grid points in the y direction: $NY = 128$). The perturbation energy of the velocity field,

$$E(\mathbf{v}) = \int_{-1}^1 \int_0^d (u^2 + v^2) dx dy, \quad (31)$$

is used to quantify the destabilizing effects of the controller. For instance, the perturbation energy of the simulation case shown in Fig. 4, whose curve can be found in Fig. 5 denoted as “ $E(\mathbf{v})$ uncontrolled”, decreases as the flow is stabilized by the imposed magnetic field.

When the control law (27) is applied to the fully established flow achieved in Fig. 3, the flow does not eventually turn stable as it is shown in Fig. 4, although the imposed magnetic field is present. The perturbation energy curve for this controlled case, presented in Fig. 5, shows that the controlled flow has much higher energy than the uncontrolled one, which eventually goes to zero (laminar flow) at $t \approx 800$. Note that the ratio between the peak control energy,

$$C(v) = \int_0^d v(x, -1, t)^2 + v(x, 1, t)^2 dx, \quad (32)$$

and the perturbation kinetic energy, $C(v)/E(v)$, is less than 4%, which suggests that small control effort can result in considerable mixing effect. Fig. 6 shows the simulation results for this controlled case, which has identical initial conditions as the one presented in Fig. 4. The rich vortex distribution greatly enhances the mixing in the fluid.

A particle tracking is carried out to further visualize the effectiveness of mixing. At the initial time, the particles are concentrated on several circular regions. Fig. 7 shows the particle map evolution when the control law (27) is applied. The enhanced mixing significantly improves the heat convection. As depicted in Fig. 8, the heat flux (represented by the boundary temperature gradient) of the controlled flow is kept on a much greater level than the uncontrolled flow, which eventually goes to the equilibrium solution in which convection vanishes. Fig. 9 shows the temperature distribution in the controlled flow. It is clear that the temperature distribution is significantly influenced by the vortices, which are not present in the uncontrolled stable flow. Note that

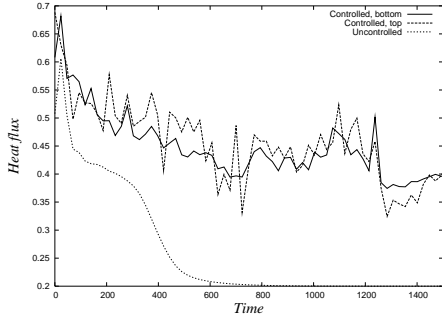


Fig. 8. Boundary heat flux ($Re = 7500$, $B_e = 0.3$)



Fig. 9. Temperature distribution ($Re = 7500$, $B_e = 0.3$, $t = 800$)

several high gradient regions, where the heat conduction is very strong, can be found near the boundaries.

A more stable flow, with $Re=4000$, is also simulated to study the effectiveness of the controller for heat transfer enhancement. In this case, the flow is stable even if the transverse magnetic field is not present. This simulation starts with a stable Hartmann equilibrium profile. Fig. 10 shows the vorticity maps for different times after the control law (27) is applied at $t = 0$. The heat flux in the controlled flow, as shown in Fig. 11, is significantly improved, while the heat flux of the uncontrolled stable flow is virtually constant (the horizontal line at $y=0.2$). The heat flux is nearly tripled when compared with the equilibrium heat flux (nearly 5 times at the peak $t \approx 400$). Fig. 12 shows the temperature distribution for this case. The similarity between the vorticity and temperature distribution suggests the enhanced mixing has a decisive influence on the heat transfer.

VIII. CONCLUSION

In this work, a nonlinear Lyapunov-based boundary feedback control law that maximizes a mixing measure, minimizing the control and sensing efforts, was designed. Considering the high dimensional and nonlinear nature of the plant being controlled, it is remarkable that the proposed controller is a simple proportional, decentralized, robust controller. The effectiveness of the optimal controller in enhancing not only mixing but also heat transfer in 2D Hartmann flow was demonstrated in numerical simulations, where it was shown that by applying boundary control intelligently in a

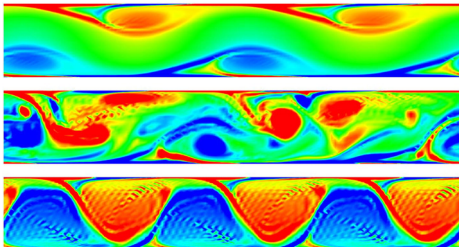


Fig. 10. Vorticity map showing flow being destabilized ($Re = 4000$, $B_e = 0.3$, $t = 373, 560, 1377$)

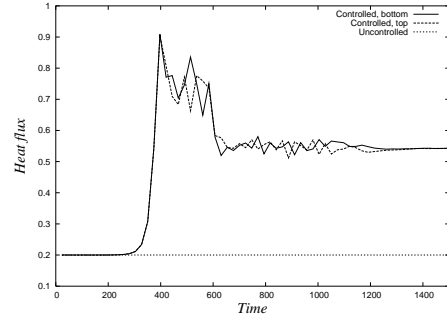


Fig. 11. Boundary heat flux ($Re = 4000$, $B_e = 0.3$)

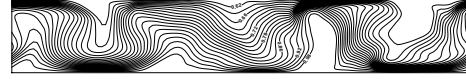


Fig. 12. Temperature distribution ($Re = 4000$, $B_e = 0.3$, $t = 800$)

feedback loop, mixing and heat transfer were considerably improved using a relatively small control effort. Unlike most control applications, the proposed controller is destabilizing. However, the controller was designed not to drive the states or control inputs unbounded but to locally destabilize the system, leading to bounded unsteadiness in the system, and, indirectly, to enhance mixing and heat transfer.

Our attempt to control the unsteadiness of the fully coupled MHD equations combined with the heat transfer equation has not been explored before. This work reveals a promising future for heat transfer enhancement via active boundary control. Attention will be given in the future to quasi-3D (flow variables are functions of two space variables but have three components) and 3D geometries.

REFERENCES

- [1] E. Spong, J. Reizes, and E. Leonardi, "Efficiency improvements of electromagnetic flow control," *Heat and Fluid Flow*, vol. 26, pp. 635–655, 2005.
- [2] H. Choi, P. Moin, and J. Kim, "Active turbulence control for drag reduction in wall-bounded flows," *J. Fluid. Mech.*, vol. 262, p. 75, 1994.
- [3] T. Berger, J. Kim, C. Lee, and J. Lim, "Turbulent boundary layer control utilizing the lorentz force," *Phys. Fluids*, vol. 12, p. 631, 2000.
- [4] J. Baker, A. Armaou, and P. Christofides, "Drag reduction in transitional linearized channel flow using distributed control," *Int. J. Control*, vol. 75, no. 15, pp. 1213–1218, 2002.
- [5] S. Singh and P. Bandyopadhyay, "Linear feedback control of boundary layer using electromagnetic microtiles," *Transactions of ASME*, vol. 119, pp. 852–858, 1997.
- [6] E. Schuster and M. Krstić, "Inverse optimal boundary control of mixing in magnetohydrodynamic channel flows," *Proceedings of the 2003 IEEE Conference on Decision and Control*, 2003.
- [7] J. Hartmann, *Theory of the laminar flow of an electrically conductive liquid in a homogeneous magnetic field*, xv(6) ed. Det Kgl. Danske Vidensk-absernes Selskab. Matematisk-fysiske Meddelelser.
- [8] O. Aamo and M. Krstic, *Flow Control by Feedback*. Springer, 2002.
- [9] R. L. Panton, *Incompressible flow*, 2nd ed. New York: Wiley, 1996.
- [10] C. Canuto, *Spectral methods in fluid dynamics*. Springer Verlag, 1998.
- [11] Y. Morinishi, T. Lund, O. Vasilyev, and P. Moin, "Fully conservative higher order finite difference schemes for incompressible flow," *Journal of Computational Physics*, vol. 143, no. 1, pp. 90–124, 1998.
- [12] J. Dukowicz and A. Dvinsky, "Approximate factorization as a high order splitting for the implicit incompressible flow equations," *Journal of Computational Physics*, vol. 102, no. 2, pp. 336–347, 1992.
- [13] T. Bewley, *Optimal and robust control and estimation of transition, convection, and turbulence*. Stanford University thesis, 1999.